



## ARTICLE

CXCR1 and CXCR2 display receptor bias for shared chemokine agonists <sup>□</sup>

Chanpreet Jassal <sup>1</sup> , Joseph Strawn <sup>1</sup>, Emily Walsh <sup>2</sup> , Krishna Rajarathnam <sup>3,\*</sup> , Sudarshan Rajagopal <sup>1,\*</sup>

<sup>1</sup> Department of Medicine, Duke University School of Medicine, Durham, North Carolina

<sup>2</sup> Trinity College of Arts and Sciences, Duke University, Durham, North Carolina

<sup>3</sup> Department of Biochemistry and Molecular Biology, Department of Microbiology and Immunology, Institute for Human Infections and Immunity, Sealy Center for Structural Biology and Molecular Biophysics, University of Texas Medical Branch, Galveston, Texas

## ARTICLE INFO

## Article history:

Received 6 October 2025

Accepted 26 February 2026

Available online 5 March 2026

## Key words:

Biased agonism

Receptor bias

Chemokine receptor

Chemokine

G protein-coupled receptor

## ABSTRACT

G protein-coupled receptors (GPCRs) mediate diverse signaling outputs through their proximal transducers: G proteins, GPCR kinases, and  $\beta$ -arrestins. Although ligand bias at chemokine receptors (CKRs), where ligands for the same receptor display distinct signaling patterns, is well recognized, receptor bias, where the same agonist at different receptors yields distinct transducer engagement, remains poorly understood. We compared endogenous chemokine ligands (CXCL1, CXCL5, CXCL7, CXCL8) at the highly homologous CXCR1 and CXCR2 using biosensor assays to measure  $G\alpha i$  activation,  $\beta$ -arrestin1/2 recruitment, GPCR kinase 2/3/5/6 translocation, and receptor internalization. Our data reveal qualitatively different signaling patterns, most notably where CXCL1 acts as a G protein-biased partial agonist at CXCR1 but as a balanced full agonist at CXCR2. These signaling differences correlate with receptor internalization but not subcellular ERK activation patterns measured using compartment-specific biosensors. Collectively, our findings demonstrate receptor bias in CKR signaling, transducer activation, and compartmentalized kinase activation in translating chemokine identity into discrete functional outcomes.

**Significance Statement:** Ligand bias, where different ligands for the same receptor display different signaling patterns, is now well appreciated. However, there are only a few examples of receptor bias, where the same agonist generates distinct signaling profiles at different receptors. This study used biosensors and compartmental ERK biosensors to show that shared ligands of CXCR1 and CXCR2 differentially engage G proteins,  $\beta$ -arrestins, and G protein-coupled receptor kinases, revealing receptor bias in CXCL1-mediated signaling that extends beyond prior characterizations.

© 2026 American Society for Pharmacology and Experimental Therapeutics. Published by Elsevier Inc. All rights are reserved, including those for text and data mining, AI training, and similar technologies.

\* Address correspondence to: Sudarshan Rajagopal, Department of Medicine, Duke University School of Medicine, Durham, NC 27710. E-mail: [sudarshan.rajagopal@duke.edu](mailto:sudarshan.rajagopal@duke.edu); or Krishna Rajarathnam, Department of Biochemistry and Molecular Biology, Department of Microbiology and Immunology, Institute for Human Infections and Immunity, Sealy Center for Structural Biology and Molecular Biophysics, University of Texas Medical Branch, Galveston, TX 77555. E-mail: [krrajara@utmb.edu](mailto:krrajara@utmb.edu)

<sup>□</sup> This article has supplemental material available at [molpharm.aspetjournals.org](http://molpharm.aspetjournals.org).

<https://doi.org/10.1016/j.molpha.2026.100117>

0026-895X/© 2026 American Society for Pharmacology and Experimental Therapeutics. Published by Elsevier Inc. All rights are reserved, including those for text and data mining, AI training, and similar technologies.

## 1. Introduction

G protein-coupled receptors (GPCRs) are the most common class of receptors found throughout the human body, and are the target of approximately 35% of all US Food and Drug Administration-approved drugs.<sup>1</sup> GPCRs mediate signaling by engaging many transducers, such as heterotrimeric G proteins, GPCR kinases (GRKs), and  $\beta$ -arrestins.<sup>2</sup> Most ligands that bind GPCRs are thought to display “balanced” agonist activity, signaling through pathways mediated by  $\beta$ -arrestins and G proteins.<sup>3</sup>

However, it has been appreciated that some receptor-ligand systems selectively signal through some pathways over others in a ligand-, receptor-, or systems-dependent manner—a phenomenon referred to as “biased agonism.”<sup>4</sup> Given the broad range of physiological processes regulated by GPCRs and the association of their dysfunction with numerous pathological conditions,<sup>5</sup> investigating biased signaling to enhance efficacy and reduce side effect profiles of existing GPCR-based therapies offers significant promise.

Moreover, GPCRs with multiple endogenous agonists can display bias between those ligands.<sup>4</sup> The human chemokine system represents a subfamily of GPCRs where endogenous bias is critical in modulating diverse cellular functions. It is composed of approximately 50 known endogenous chemokine ligands and 20 known chemokine receptors (CKRs), displaying a spectrum of selective and promiscuous interactions at both the ligand and receptor level, resulting in biased responses.<sup>6</sup> Biased agonism, specifically ligand bias, in the chemokine system was first described at CCR7, where studies demonstrated selective signaling through either  $\beta$ -arrestins or G proteins.<sup>7–9</sup> Later, it was appreciated that some CKRs, such as ACKR3, also known as CXCR7, are  $\beta$ -arrestin-biased and signal exclusively through  $\beta$ -arrestin in the absence of G protein activation.<sup>10</sup> However, the complexity of biased agonism at CKRs remains to be fully characterized. This is especially true of receptor bias, the ability of the same agonist to result in distinctly different signaling patterns depending on the receptor to which it binds.<sup>4</sup>

C-X-C motif chemokine receptor 1 (CXCR1) and C-X-C motif chemokine receptor 2 (CXCR2) are the major CKRs expressed on neutrophils and mediate their recruitment to infection sites to trigger cytotoxic effects.<sup>11</sup> CXCR1 and CXCR2 are highly homologous and share 77% amino acid identity with a majority of the divergent residues clustered in 3 regions: (1) the N-terminal segment before transmembrane domain 1, (2) the region from transmembrane domain 4 to the end of the second extracellular loop, and (3) the C-terminal cytoplasmic tail.<sup>12,13</sup> Although it is well established that CXCR1 and CXCR2 are high-affinity receptors for CXCL8, they also bind 6 additional chemokines (CXCL1–3, 5–8) with varying affinities.<sup>14,15</sup> These chemokines share the characteristic Glu-Leu-Arg (ELR) motif at the N terminus that is critical for activating both receptors. Although studies have focused on ligand bias between these chemokines at either CXCR1 and CXCR2,<sup>14–16</sup> little is known regarding the presence of receptor bias in the response of the same chemokine agonist between these 2 closely related receptors. Toward this goal, we characterized how biased signaling at CXCR1 and CXCR2 receptors and their endogenous chemokines, CXCL1, CXCL5, CXCL7, and CXCL8, influences unique intracellular signaling events through  $\beta$ -arrestins, G proteins, and GRK transducers.

## 2. Materials and methods

### 2.1. Generation of constructs

Construct cloning was performed using conventional techniques such as overlap cloning, as previously described, unless otherwise indicated.<sup>17</sup>

### 2.2. Bacterial strains

XL-10 Gold ultracompetent *Escherichia coli* (Agilent) was used to express all constructs used in this manuscript (Supplemental Table 1).

### 2.3. Cell culture and transfection

Human embryonic kidney (WT HEK293T,  $\beta$ -arrestin 1/2 knockout [KO]) cells were grown in minimum essential media (MEM) supplemented with 10% FBS and 1% penicillin/streptomycin (P/S) at 37 °C and 5% CO<sub>2</sub>.  $\beta$ -arrestin 1/2 CRISPR KO cells were provided by Stephane Laporte (McGill University, Montreal, Quebec, Canada).<sup>18</sup> CRISPR/Cas9-edited HEK293A GRK KO cells ( $\Delta$ GRK2/3/5/6) were provided by Asuka Inoue, Tohoku University, Japan.<sup>19</sup> Cultured cells were routinely checked for possible mycoplasma contamination. For bioluminescence resonance energy transfer (BRET) and luminescence-based assays, transient transfections were performed using the polyethylenimine (PEI) transfection method. Cell culture media was replaced 30 minutes prior to transfection. Plasmid constructs were suspended in Opti-MEM (GIBCO) to a final volume of 100  $\mu$ L. In a separate tube, 100  $\mu$ L of PEI in Opti-MEM was prepared at a PEI: DNA ratio of 3:1 using a PEI stock concentration of 1 mg/mL. After 5 minutes, the PEI solution was added to the plasmid DNA, gently mixed, and allowed to incubate at room temperature for 30 minutes. The PEI: DNA mixture was then added to the cells.

### 2.4. TRUPATH G protein activation assays

HEK293T cells seeded in 6-well plates were transiently transfected using PEI with wild-type CXCR1 or CXCR2, *Gai1*-RLuc8, *G $\gamma$ 9*-GFP2, and *G $\beta$ 3* at equal amounts.<sup>20</sup> Twenty-four hours later, cells were plated onto clear-bottom, white-walled, 96-well plates (Costar) at 100,000 cells/well in clear MEM supplemented with 1% FBS and 1% P/S. The following day, the media were aspirated, and cells were incubated at room temperature with 80  $\mu$ L of coelenterazine 400a (5  $\mu$ M final concentration) in Hanks' balanced salt solution (HBSS) (Gibco) supplemented with 20 mM HEPES for 5 minutes. BRET signals were measured with a BioTek Synergy Neo2 plate reader at 37 °C plates with a standard 410 / 80 nm wavelength filter (*Renilla* luciferase [RLuc]) and 515 / 30 nm wavelength filter following the addition of 20  $\mu$ L of ligands (10  $\mu$ M of chemokines). BRET ratios were calculated by dividing the 510 nm signal by the 400 nm signal. Net BRET values were calculated by subtracting the vehicle BRET ratio from the ligand-stimulated BRET ratio.

### 2.5. ERK activity reporter BRET assays

HEK293T cells seeded in 6-well plates were transiently transfected using PEI with wild-type CXCR1 or CXCR2, ERK activity reporter BRET biosensors tagged to different cellular locations, and dynamin K44A or pcDNA control. Twenty-four hours later, cells were plated onto clear-bottom, white-walled, 96-well plates (Costar) at 100,000 cells/well in clear MEM supplemented with 1% FBS and 1% P/S with or without 200 ng/mL pertussis toxin (PTX). The following day, the media were aspirated, and cells were incubated at room temperature with 80  $\mu$ L of coelenterazine h (2.5  $\mu$ M final concentration) in HBSS supplemented with 20 mM HEPES for 5 minutes. BRET signals were measured with a BioTek Synergy Neo2 plate reader at 37 °C using a 460  $\pm$  40 nm wavelength filter (NanoLuc luciferase) and a 540  $\pm$  25 nm wavelength filter (mVenus). Three prereads were taken to quantify the baseline BRET signals before 20  $\mu$ L of ligands were added (10  $\mu$ M of chemokines). BRET ratios were calculated by dividing the 530 nm signal by the 480 nm signal. Net BRET values were calculated by subtracting the vehicle BRET ratio from the ligand-stimulated BRET ratio.

## 2.6. $\beta$ -arrestin recruitment and receptor internalization BRET assays

HEK293T and  $\beta$ -arrestin 1/2 KO cells seeded in 6-well plates were transiently transfected using PEI with CXCR1/CXCR2 tagged with a C-terminal RLuc8, and  $\beta$ -arrestin1 or  $\beta$ -arrestin2 tagged with a C-terminal YFP for  $\beta$ -arrestin recruitment assays or FYVE-tagged mVenus for receptor internalization. Twenty-four hours later, cells were plated onto clear-bottom, white-walled, 96-well plates (Costar) at 100,000 cells/well in clear MEM supplemented with 1% FBS and 1% P/S with or without 200 ng/mL PTX. The following day, the media were aspirated, and cells were incubated at room temperature with 80  $\mu$ L of coelenterazine h (2.5  $\mu$ M final concentration) in HBSS supplemented with 20 mM HEPES for 5 minutes. BRET signals were measured with a BioTek Synergy Neo2 plate reader at 37 °C using a 460  $\pm$  40 nm wavelength filter (RLuc) and a 540  $\pm$  25 nm wavelength filter (mVenus). Three prereads were taken to quantify the baseline BRET signals before 20  $\mu$ L of ligands were added (10  $\mu$ M of chemokines). BRET ratios were calculated by dividing the 530 nm signal by the 480 nm signal. Net BRET values were calculated by subtracting the vehicle BRET ratio from the ligand-stimulated BRET ratio.

## 2.7. NanoLuc binary technology GRK recruitment assays

HEK293T cells seeded in 6-well plates were transiently transfected using PEI with wild-type CXCR1 or CXCR2; GRK2/GRK3/GRK5/GRK6 were tagged with a C-terminal LgBiT,<sup>19</sup> and a CD8 $\alpha$ -SmBiT (plasma membrane marker). Twenty-four hours after transfection, cells were plated onto clear-bottom, white-walled, 96-well plates (Costar) at 100,000 cells/well in clear MEM supplemented with 1% FBS and 1% P/S with or without 200 ng/mL PTX. The following day, the media were aspirated, and cells were incubated at room temperature with 80  $\mu$ L of coelenterazine h (2.5  $\mu$ M final concentration) in HBSS Gibco supplemented with 20 mM HEPES for 5 minutes. Luminescence signals were read using a BioTek Synergy Neo2 plate reader at 37 °C, without a wavelength-specific filter. Three prereads were taken to quantify the baseline luminescence before adding 20  $\mu$ L of ligands at the appropriate concentrations. The average of the luminescence prereads was divided from each read following ligand addition to calculate a change in luminescence over baseline and then normalized to vehicle treatment.

## 2.8. CXCR1 and CXCR2 ligands

All chemokines were recombinantly expressed as fusion proteins from the pET32 Xa/LIC plasmid, with the chemokine gene inserted at the ligation-independent cloning site. The plasmids were transformed into *E. coli* BL21(DE3) cells (Invitrogen) and cultured in LB medium. Briefly, the transformed cells were grown to an  $A_{600}$  of ~0.6 and induced with 0.2 to 1 mM IPTG for 6 hours at 37 °C or 20 hours at 25 °C. Fusion proteins from lysed cells were purified using a nickel–nitrilotriacetic acid column, cleaved with Factor Xa (Novagen), and further purified by reverse-phase high-performance liquid chromatography. Protein purity and molecular mass were confirmed by SDS-PAGE and MALDI-TOF mass spectrometry. The chemokines were diluted in Dulbecco's PBS supplemented with 0.1% bovine serum albumin, and aliquots were stored at –80 °C until needed for use.

## 2.9. Statistical analyses

Statistical analyses were performed using GraphPad Prism 10 (GraphPad Software). Values are reported as mean  $\pm$  SD. Dose-response curves were fitted to a log agonist versus stimulus with

3 parameters (span, baseline, and EC<sub>50</sub>) with the minimum baseline corrected to zero. For concentration-response experiments, a two-way ANOVA was used to independently assess the effects of ligand identity and concentration, as well as their interaction, across all 4 ligands. A significant ligand and concentration interaction was interpreted as evidence that concentration-response profiles differed between ligands. If such an interaction was observed ( $P < .05$ ), follow-up two-way ANOVAs were performed between individual ligand pairs to identify specific differences in response profiles across concentrations, with correction for multiple comparisons. For time course experiments, pairwise comparison using a one-way ANOVA followed by Tukey's multiple comparison test was conducted on the area under the curve.  $P < .05$  was considered to be statistically significant. All experiments and statistical analyses were conducted in an exploratory framework to identify and compare signaling trends across ligands and receptors, without a prespecified formal null hypothesis. Reported  $P$  values are intended to be descriptive rather than to support formal hypothesis testing. Further details of statistical analysis and replicates are reported in the figure legends. Bias plots were generated using normalized dose-response data for G protein activation,  $\beta$ -arrestin1 and  $\beta$ -arrestin2 recruitment, and receptor internalization, and plotting responses at the same concentration of chemokine for each set of analyses.

## 3. Results

### 3.1. Chemokines promote differential activation of G proteins and $\beta$ -arrestins at CXCR1 and CXCR2

We first assessed G protein signaling activity at CXCR1 and CXCR2 with 4 endogenous chemokine ligands—CXCL1, CXCL5, CXCL7, and CXCL8. Using the TRUPATH BRET assay<sup>20</sup> (Fig. 1A), we assessed CXCR1 and CXCR2 signaling by measuring heterotrimeric G $\alpha$ i dissociation. Following chemokine stimulation of CXCR1, CXCL8 was most effective at G protein activation, followed by CXCL7, CXCL1 and CXCL5 (Fig. 1B). In contrast, although every chemokine promoted G $\alpha$ i activity at CXCR2, no differences in maximal response between ligands were observed (Fig. 1C). Given the role of  $\beta$ -arrestin2 in desensitizing G protein signaling, we next examined  $\beta$ -arrestin2 recruitment to CXCR1 and CXCR2 following chemokine stimulation by BRET (Fig. 1D). At CXCR1, all ligands recruited  $\beta$ -arrestin2 (Fig. 1E) with rank order of CXCL8 > CXCL7 > CXCL1 > CXCL5 (Fig. 1, F and G). In contrast, at CXCR2, both CXCL8 and CXCL1 generated maximal responses, closely followed by CXCL7, and then CXCL5, which showed the lowest  $\beta$ -arrestin2 activity (Fig. 1, H–J). Similar trends were observed with  $\beta$ -arrestin1 recruitment for all chemokines at both CXCR1 and CXCR2 (Supplemental Fig. 1, A–D).

Given that CXCR1 and CXCR2 are frequently coexpressed and have been reported to interact,<sup>21</sup> we investigated whether their coexpression alters  $\beta$ -arrestin2 recruitment. Trends were consistent with our previous findings for each receptor expressed individually, with CXCL8 eliciting the greatest  $\beta$ -arrestin2 recruitment at CXCR1 relative to all other chemokines, and CXCL1 inducing levels of maximal  $\beta$ -arrestin2 recruitment comparable to CXCL8 at CXCR2 (Supplemental Fig. 1, E–H).

### 3.2. CXCR1 and CXCR2 generate distinct patterns of GRK recruitment to the plasma membrane

We next examined GRK2/GRK3 and GRK5/GRK6 recruitment to the plasma membrane marker CD8 $\alpha$  using a previously validated NanoLuc binary technology complementation assay<sup>19,22</sup> (Fig. 2A) following stimulation of CXCR1 and CXCR2. Upon activation of

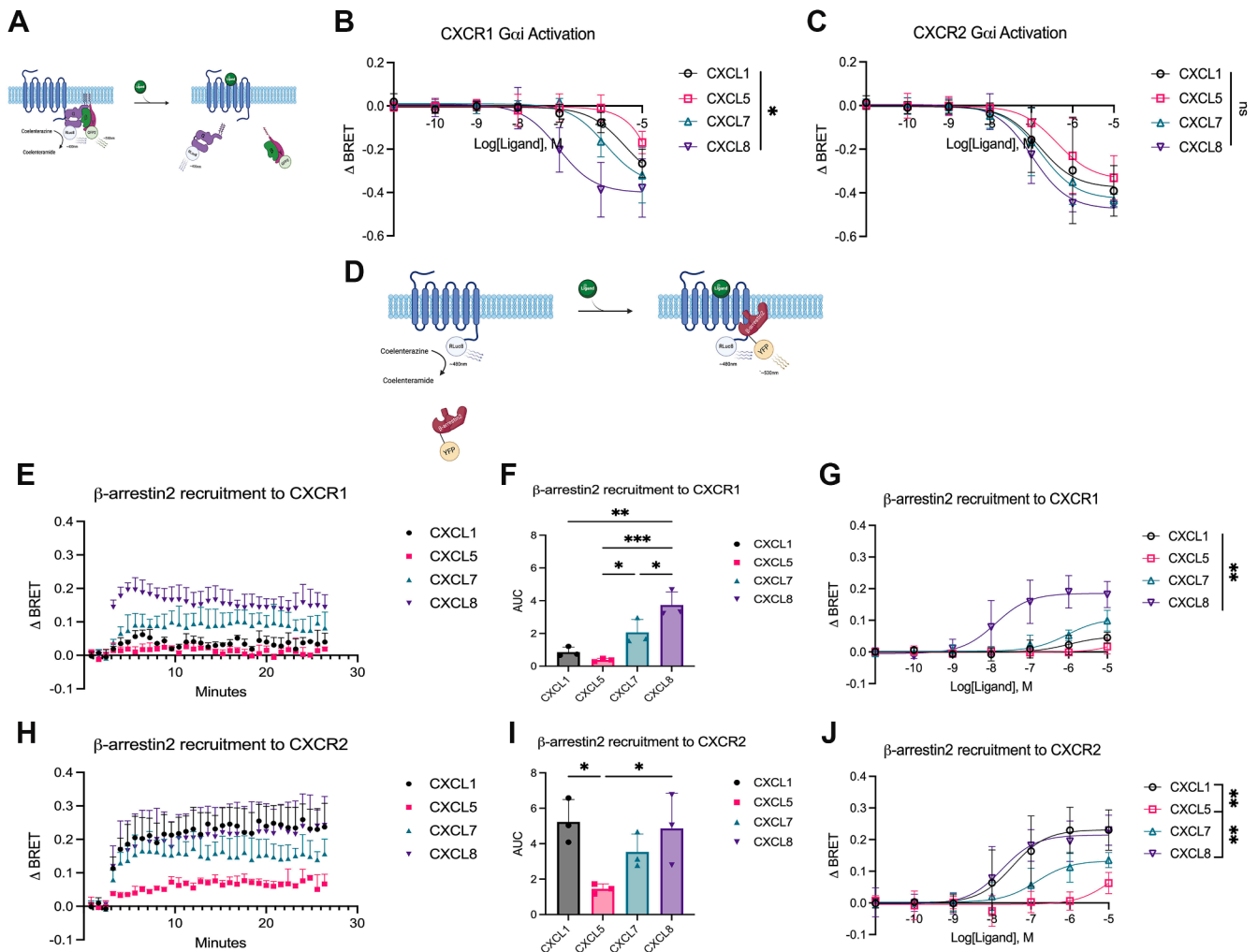


**Fig. 1.** G protein dissociation and  $\beta$ -arrestin 2 recruitment to CXCR1 and CXCR2. (A) Schematic of BRET-based TRUPATH assay to assess G protein dissociation. (B and C) Dose-response curves of G protein dissociation following receptor activation in HEK293T cells transiently expressing CXCR1 and CXCR2 at the listed concentration of chemokine. (D) Schematic of BRET-based assay to monitor  $\beta$ -arrestin recruitment to receptor in HEK293T cells transiently expressing  $\beta$ -arrestin2-YFP and either CXCR1-RLuc8 or CXCR2-RLuc8. (E) Time course data of  $\beta$ -arrestin2 recruitment to CXCR1 following 10  $\mu$ M chemokine stimulation (F) with corresponding area under the curve (AUC) quantification. (G) Agonist dose-dependent responses of  $\beta$ -arrestin2 recruitment to CXCR1. (H) Time course data of  $\beta$ -arrestin2 recruitment to CXCR2 following 10  $\mu$ M chemokine stimulation (I) with corresponding AUC quantification. (J) Agonist dose-dependent responses of  $\beta$ -arrestin2 recruitment to CXCR2. Data for (B and C) are measured between 1 and 2 minutes following chemokine addition and are the mean  $\pm$  SD,  $n = 3$  independent plate-based experiments. Data for (E–J) are the mean  $\pm$  SD ( $n = 3$ ) of independent plate-based experiments. For (F and I), a one-way ANOVA followed by Tukey's multiple comparison test was used to compare different chemokine treatments, and for (B), (C), and (G–J), a two-way ANOVA was used. ns:  $P \geq .05$ , \* $P < .05$ ; \*\* $P < .005$ ; \*\*\* $P < .0005$ ; \*\*\*\* $P < .0001$  denotes a significant effect of the ligand by one-way or two-way ANOVA. Created in BioRender. Jassal, C. (2026) <https://BioRender.com/bz55qly3>.

CXCR1, chemokine-induced recruitment of GRK2 and GRK3 mirrored the patterns observed in the  $\beta$ -arrestin2 recruitment assay, with CXCL8 promoting rapid and maximal recruitment followed by CXCL7, then CXCL1 and CXCL5 (Fig. 2, B and F). A similar pattern was observed with GRK3 (Fig. 2, C and G). Statistically significantly lower recruitment was seen for GRK5 (Fig. 2, D and H) and GRK6 (Fig. 2, E and I), likely due to higher basal signal from the kinase already localized to the plasma membrane.<sup>22</sup> A similar pattern was seen for GRK5/6 compared to GRK2/3, with notable recruitment promoted by CXCL7 and CXCL8 compared to CXCL1 and CXCL5. Interestingly, at CXCR2, each GRK examined displayed comparable levels of plasma membrane recruitment following stimulation across all 4 chemokines (Fig. 2, J–Q).

To evaluate the role of G protein activation in recruiting GRKs to the plasma membrane, we used PTX to inhibit G $\alpha$ i activation. Following stimulation with CXCL8, we found that PTX statistically significantly reduced both CXCR1- and CXCR2-mediated

recruitment of GRK2 and GRK3 (Supplemental Fig. 2, E and G). These findings corroborate previous reports that the activity of GRK2/3 family members is largely, but not entirely, dependent on G protein activation due to the presence of a PH domain recognizing free G $\beta\gamma$  following G protein activation.<sup>23</sup> Interestingly, GRK6 recruitment following CXCR2 activation was statistically significantly increased upon PTX treatment (Supplemental Fig. 2H).

To investigate the functional consequences of GRKs, we employed a previously validated CRISPR/Cas9-edited HEK293 cell line lacking GRK2, GRK3, GRK5, and GRK6 ( $\Delta$ GRK2/3/5/6)<sup>19</sup> and examined  $\beta$ -arrestin2 recruitment to CXCR1 and CXCR2 by BRET following chemokine stimulation and selective rescue of GRK2 or GRK5 (Supplemental Fig. 3). GRK2 rescue enhanced  $\beta$ -arrestin2 recruitment to CXCR1 for all agonists, whereas GRK5 rescue only had a significant effect with CXCL7. The magnitude of the effect of GRK2 rescue was relatively small except at CXCL7 and CXCL8. A different pattern was observed at CXCR2. Similar to CXCR1, GRK2

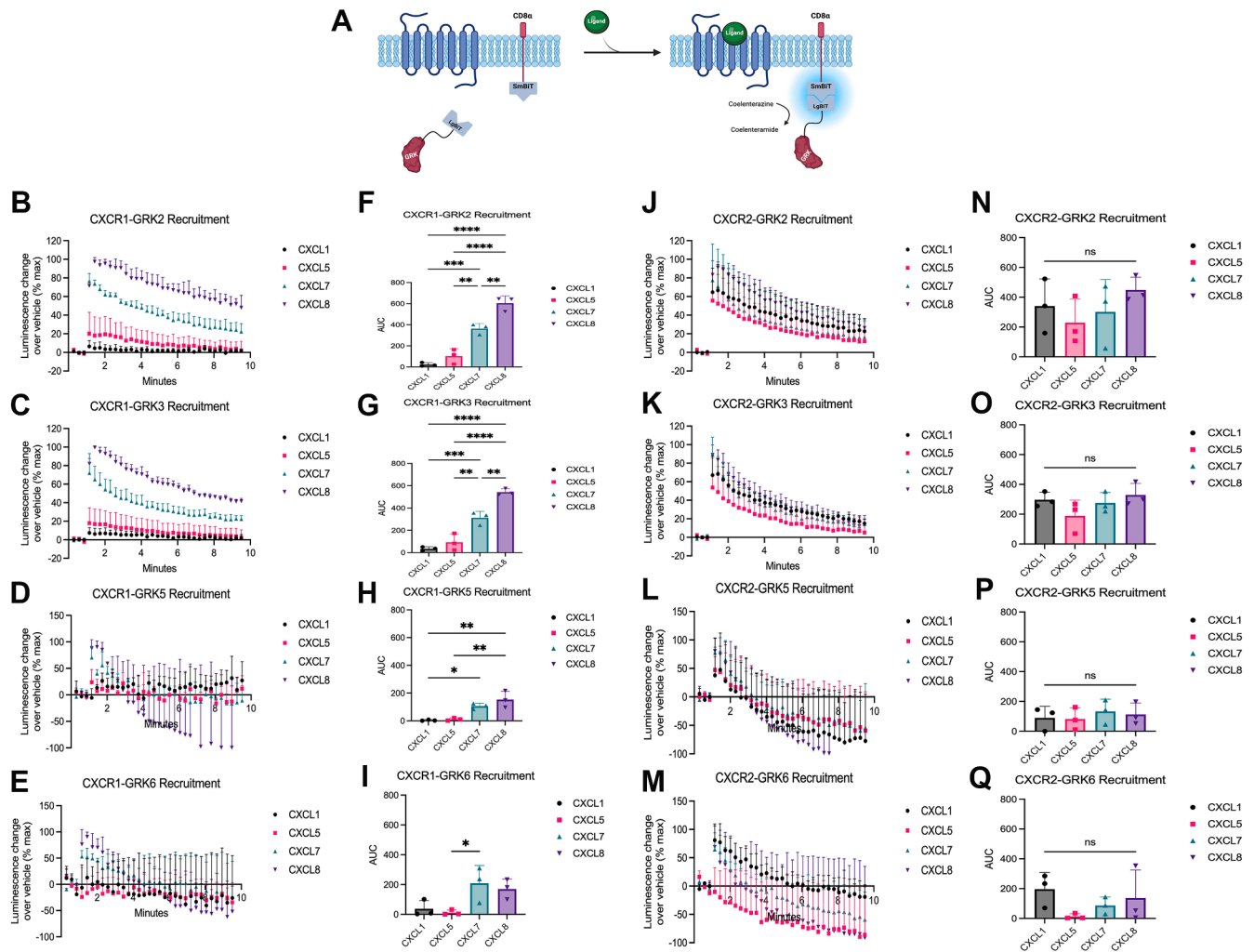


**Fig. 2.** GRK recruitment to plasma membrane following activation of CXCR1 and CXCR2. (A) Schematic of NanoLuc binary technology (NanoBiT) luciferase assay to assess GRK recruitment to the plasma membrane using GRK-LgBiT and CD8 $\alpha$ -SmBiT constructs in HEK293T cells transiently expressing either CXCR1 or CXCR2. (B–E) Time course data of GRK2, GRK3, GRK5, and GRK6 recruitment upon activation of CXCR1 with 10  $\mu$ M of chemokine (F–I) with corresponding area under the curve (AUC) quantification. (J–M) Time course data of GRK2, GRK3, GRK5, and GRK6 recruitment upon activation of CXCR2 with 10  $\mu$ M of chemokine (N–Q) with corresponding AUC quantification. Data for (B–Q) are the mean  $\pm$  SD ( $n = 3$ ) of independent plate-based experiments. For (F–I) and (N–Q), a one-way ANOVA followed by Tukey's multiple comparison test was used to compare different chemokine treatments. ns:  $P \geq .05$ ; \* $P < .05$ ; \*\* $P < .005$ ; \*\*\* $P < .0005$ ; \*\*\*\* $P < .0001$  denotes a significant effect of the ligand by one-way ANOVA. Created in BioRender. Jassal, C. (2026) <https://BioRender.com/imzomh6>.

rescue produced statistically significant increases in  $\beta$ -arrestin2 recruitment for all agonists; however, GRK5 rescue led to statistically significant increases in  $\beta$ -arrestin2 recruitment in response to CXCL1 and CXCL5 (rather than CXCL7 at CXCR1) compared with the pcDNA3.1 control. These findings demonstrate that GRKs have distinct agonist-specific effects on CXCR1 and CXCR2 engagement with  $\beta$ -arrestin2.

### 3.3. Chemokines promote different amounts of CXCR1 and CXCR2 internalization

To determine the functional relevance of the trends observed in  $\beta$ -arrestin2 and GRK recruitment, we next assessed agonist-induced internalization of CXCR1 and CXCR2. Receptor internalization was monitored by BRET between luciferase-tagged CXCR1 and CXCR2 as they traffic to early endosomes with an FYVE domain-tagged mVenus (Fig. 3A), or away from the plasma membrane using a Myrpal-tagged mVenus (Supplemental Fig. 4). At CXCR1, the rank order of early endosome association mirrored the trends observed in  $\beta$ -arrestin and GRK2/3 recruitment—CXCL8 > CXCL7 > CXCL1 ~ CXCL5

(Fig. 3, B–D). Similarly, CXCL8 promoted a statistically significant amount of CXCR1 translocation from the plasma membrane compared to CXCL1, CXCL5, and CXCL7 (Supplemental Fig. 4, A and B). However, at CXCR2, the differences between CXCL1 and CXCL8 were statistically insignificant. CXCL5 promoted statistically significantly less early endosome association (Fig. 3, E–G) and translocation from the plasma membrane (Supplemental Fig. 4, C and D), a trend consistent with the pattern of  $\beta$ -arrestin2 recruitment to CXCR2 (Fig. 11).

Given these observations, we sought to determine the role of  $\beta$ -arrestins in promoting internalization of CXCR1 and CXCR2 following treatment with CXCL8 in  $\beta$ -arrestin 1/2 KO cells. Compared to our findings in HEK293T cells, internalization of both receptors was statistically significantly reduced, but not completely abrogated (Supplemental Fig. 4, E and F). To validate receptor internalization occurs independent of G protein activation, we repeated these internalization studies in  $\beta$ -arrestin 1/2 KO cells treated with PTX; no differences in CXCR1 and CXCR2 internalization upon stimulation with CXCL8 were observed (Supplemental Fig. 4, E and F). Together, our findings suggest that

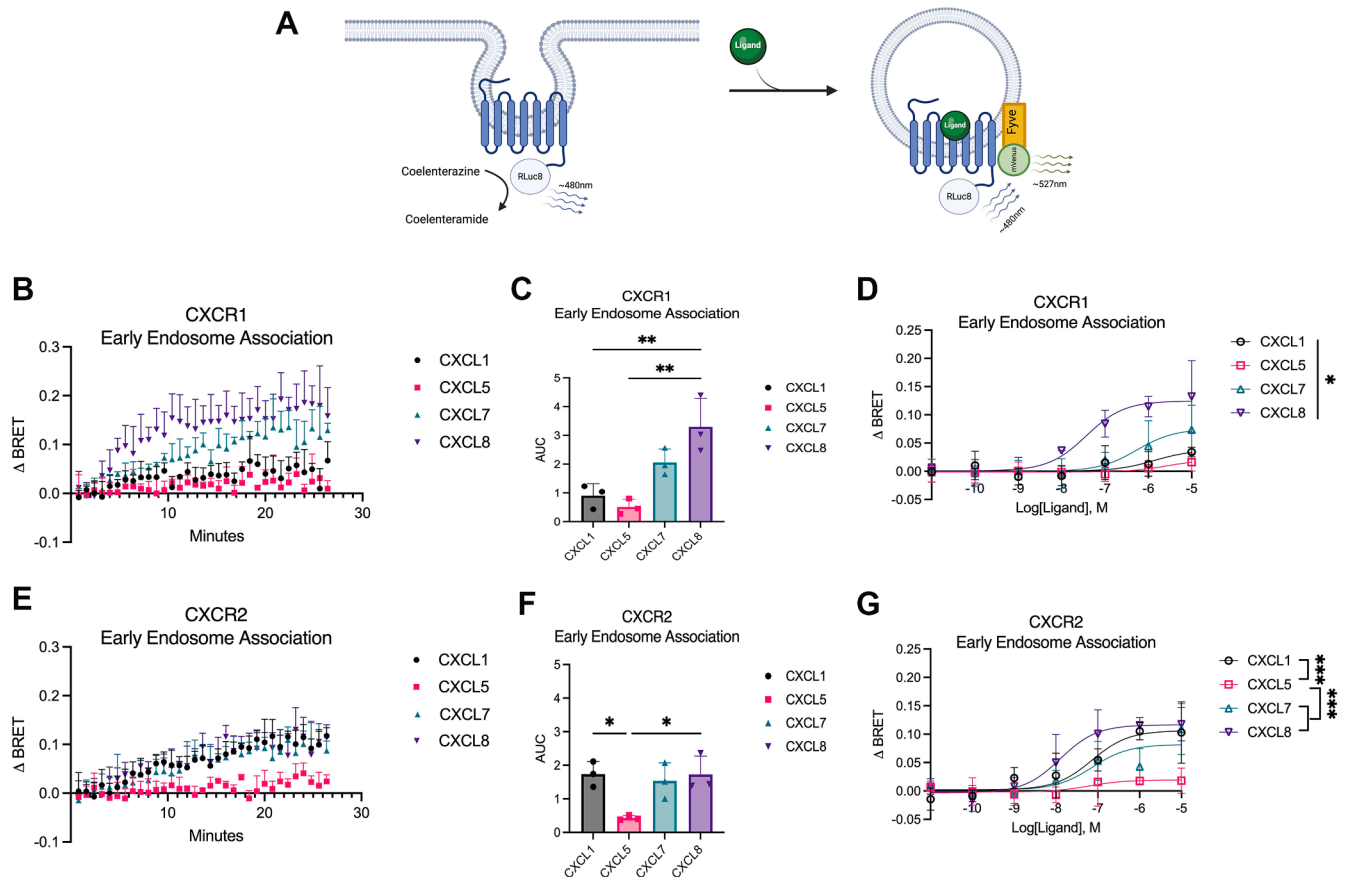


**Fig. 3.** CXCR1 and CXCR2 trafficking to early endosomes after agonist stimulation. (A) Schematic of BRET-based assay to monitor receptor trafficking to early endosomes using the BRET acceptor Fyve-mVenus in HEK293T cells transiently expressing either CXCR1-RLuc8 or CXCR2-RLuc8. (B) Time course data of CXCR1-RLuc8 trafficking to early endosomes following stimulation with 10  $\mu$ M of chemokine (C) with corresponding area under the curve (AUC) quantification. (D) Agonist dose-dependent responses of CXCR1-RLuc8 internalization between 10 and 11 minutes after ligand addition are shown and are the mean  $\pm$  SD ( $n = 3$ ) of independent plate-based experiments. (E) Time course data of CXCR2-RLuc8 trafficking to early endosomes following stimulation with 10  $\mu$ M of chemokine (F) with corresponding AUC quantification. (G) Agonist dose-dependent responses of CXCR2-RLuc8 internalization between 25 and 26 minutes after ligand addition are shown and are the mean  $\pm$  SD ( $n = 3$ ) of independent plate-based experiments. For (C) and (F), a one-way ANOVA followed by Tukey's multiple comparison test was used to compare different chemokine treatments, and for (D) and (G), a two-way ANOVA was used. ns:  $P \geq .05$ ; \* $P < .05$ ; \*\* $P < .005$ ; \*\*\* $P < .0005$ ; \*\*\*\* $P < .0001$  denotes a significant effect of the ligand by one-way or two-way ANOVA. Created in BioRender. Jassal, C. (2026) <https://BioRender.com/8tssbzzr>.

chemokine-induced internalization of CXCR1 and CXCR2 is primarily mediated by  $\beta$ -arrestins.

### 3.4. Assessment of ligand bias at CXCR1 and CXCR2

To perform a qualitative analysis of bias,<sup>24</sup> we constructed “bias plots” to identify biased agonists for each chemokine at CXCR1 and CXCR2. Bias plots allow for an assessment of assay amplification by converting dose-response data for 2 signaling pathways of interest and plotting the responses of these 2 different assays at the same concentration of ligand against each other. The resulting curve shape allows for a direct comparison of signaling through the 2 different pathways that vary depending on the sensitivities of the assays being compared; thus, “test” agonists must be qualitatively compared to a balanced reference agonist.<sup>24</sup> We compared G protein dissociation,  $\beta$ -arrestin 1 and  $\beta$ -arrestin 2 recruitment, and receptor internalization. Using CXCL8 as the reference balanced agonist, as it robustly signals through both G protein and  $\beta$ -arrestins, CXCL7 demonstrated a relative decrease in both G protein activation and  $\beta$ -arrestin coupling and internalization, acting as a partial biased agonist at CXCR1. Conversely, CXCL1 and CXCL5 displayed relative bias toward G protein activation compared to CXCL7 and CXCL8 (Fig. 4, A–C). At CXCR2, we observed a shift in

these trends. Although CXCL7 and CXCL8 acted as balanced agonists and CXCL5 as a G protein–biased agonist, CXCL1 demonstrated an appreciable shift toward  $\beta$ -arrestin coupling and internalization while preserving its ability to activate G protein (Fig. 4, D–F). Although CXCL1 is a relatively G protein–biased partial agonist at CXCR1, it behaves as a balanced full agonist similar to CXCL8 at CXCR2.

### 3.5. CXCR1 and CXCR2 activate distinct subcellular pools of ERK

Lastly, to assess whether presence of receptor bias influences distal signaling downstream of CXCR1 and CXCR2, we examined activation of the mitogen-activated protein kinase pathway through ERK1/2 phosphorylation (pERK) at different subcellular locations using previously validated BRET-based ERK activity reporter biosensors targeted to the cytoplasm, nucleus, and early endosomes<sup>25</sup> (Fig. 5A). Interestingly, although both CXCR1 and CXCR2 activated ERK in the cytoplasm (Fig. 5, B–E), nucleus (Fig. 5, F–I), and endosomes (Fig. 5, J–M), no statistically significant differences were observed across chemokines. To further dissect the role of  $\beta$ -arrestin–mediated internalization and G protein activation in promoting ERK activity, we inhibited receptor internalization using a dominant-negative mutant of the GTPase dynamin (dynamin K44A), which is required for

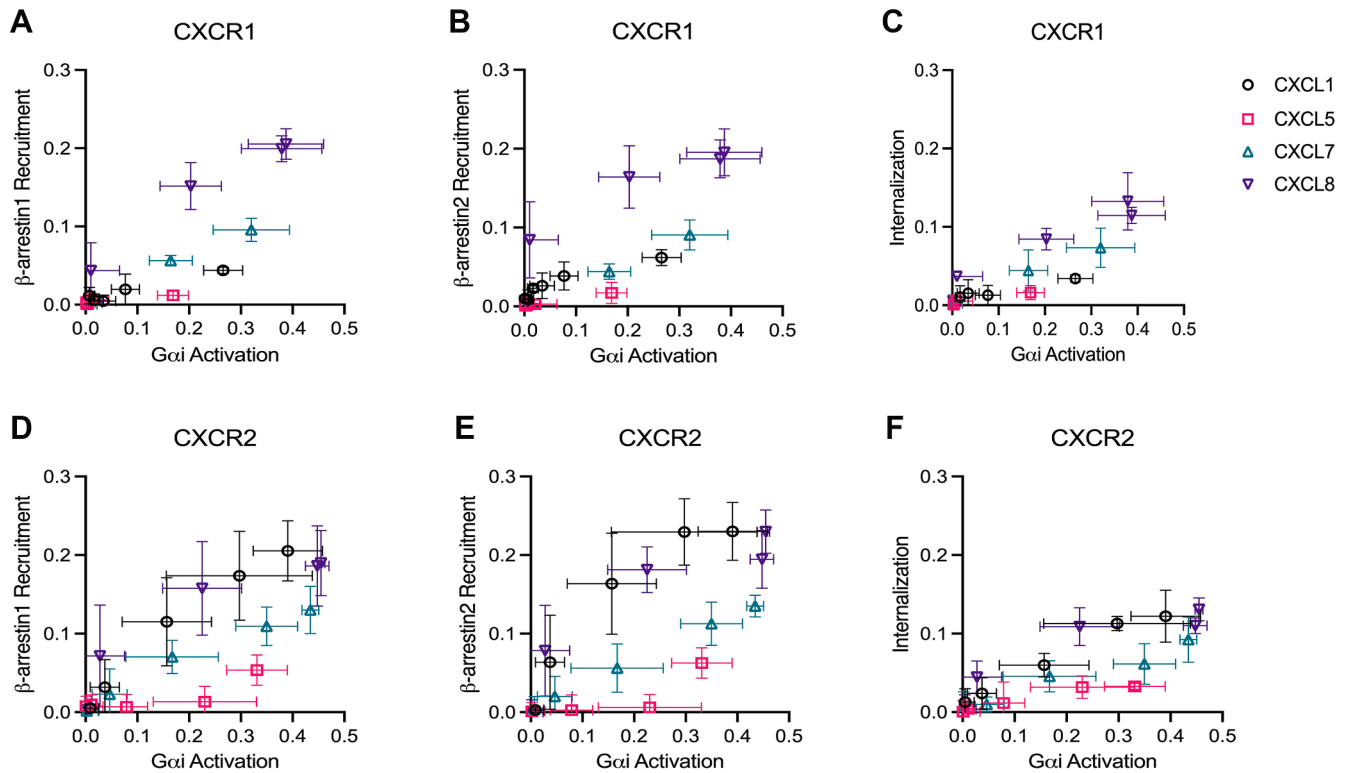


**Fig. 4.** Bias plots to qualitatively assess relative bias across signaling pathways at CXCR1 and CXCR2. CXCR1 bias plots of (A)  $\beta$ -arrestin1 recruitment and Gai activation; (B)  $\beta$ -arrestin2 recruitment and Gai activation; and (C) internalization and Gai activation. CXCR2 bias plots of (D)  $\beta$ -arrestin1 recruitment and Gai activation; (E)  $\beta$ -arrestin2 recruitment and Gai activation; and (F) internalization and Gai activation. In these plots, significant variations in the relationship between the signaling axes of the agonists are consistent with the presence of bias. In this case, CXCL8 displays relatively increased  $\beta$ -arrestin recruitment relative to Gai activation compared to other agonists (A and B), while both CXCL1 and CXCL8 display relatively increased  $\beta$ -arrestin recruitment relative to Gai activation compared to other agonists (D and E).

clathrin-mediated endocytosis,<sup>26</sup> along with PTX to inhibit G protein activation. Following treatment of CXCR1 and CXCR2 with the full endogenous agonist CXCL8, PTX treatment alone statistically significantly decreased endosomal ERK activity compared to pcDNA control at CXCR1 (Supplemental Fig. 5). However, inhibition of internalization alone had a notable effect on endosomal ERK activity at CXCR2. Simultaneous inhibition of both G proteins and internalization led to a decrease in ERK activation at CXCR2, suggesting that  $\beta$ -arrestin-mediated internalization but not G protein activation is required for maximal endosomal ERK activity at CXCR2, whereas G protein activation primarily mediates endosomal ERK activity at CXCR1. These observations validate previous findings,<sup>27</sup> which suggested that CXCR1 stabilizes a receptor signaling state at the plasma membrane, while CXCR2 promotes sustained ERK activation via G protein-dependent and G protein-independent modes at the plasma membrane and following internalization, respectively.

#### 4. Discussion

In this study, we observe that the same chemokine agonists for CXCR1 and CXCR2 display different patterns of transducer and effector activation. ELR-chemokines play diverse roles, including in normal homeostasis, combating bacterial infections in most organs, and are also selectively expressed in response to different insults in different organs.<sup>28</sup> For instance, CXCL8 is preferentially expressed in lung infections, and CXCL7 is highly expressed and released from platelets, regulating neutrophil-platelet crosstalk and thrombosis-related diseases. The receptors are predominantly expressed in neutrophils but also in nonimmune cells. Our current study characterizing the activity of proximal transducers suggests that chemokines are not

redundant, their functional phenotype is unique, and that detailed knowledge of receptor-specific signaling activities mediated by intracellular signaling machinery in conjunction with their expression levels and tissue locations is essential to fully understand the role of signaling bias in determining chemokines' role in physiology and pathology.

The most notable difference was the pattern of signaling by CXCL1, which demonstrated clear evidence of receptor bias between CXCR1 and CXCR2. At CXCR1, CXCL8 robustly activated more Gai than CXCL1, CXCL5, and CXCL7. Similarly, in rank order, CXCL8, followed by CXCL7, CXCL1, and CXCL5, recruited both  $\beta$ -arrestin1 and  $\beta$ -arrestin2. Interestingly, a different pattern was observed at CXCR2. At CXCR2, CXCL1 demonstrated a  $\beta$ -arrestin recruitment pattern similar to CXCL8. At both receptors, the patterns of receptor internalization mirrored their patterns of  $\beta$ -arrestin recruitment. It is important to note that  $\beta$ -arrestins are largely, but not entirely, responsible for mediating receptor internalization, as shown in our studies using  $\beta$ -arrestin 1/2 KO cells. Using bias plots to assess these chemokine signaling profiles, we found that CXCL1 behaves as a G protein-biased partial agonist similar to CXCL5 and CXCL7 at CXCR1, but as a balanced full agonist similar to CXCL8 at CXCR2. Our findings at CXCR1 are consistent with a recent report<sup>15</sup> that identified CXCL7, a high-affinity ligand, and CXCL1 and CXCL5, low-affinity ligands, as G protein-biased compared to the reference ligand, CXCL8. Notably, previous studies investigating ligand bias at CXCR2 concluded CXCL1 to be G protein-biased when compared to CXCL8,<sup>14,16</sup> whereas we found that CXCL1 behaved as a balanced agonist similar to CXCL8. It is important to note that bias plots are not without limitations, because factors such as system bias may still qualitatively change relative differences observed between pathways.

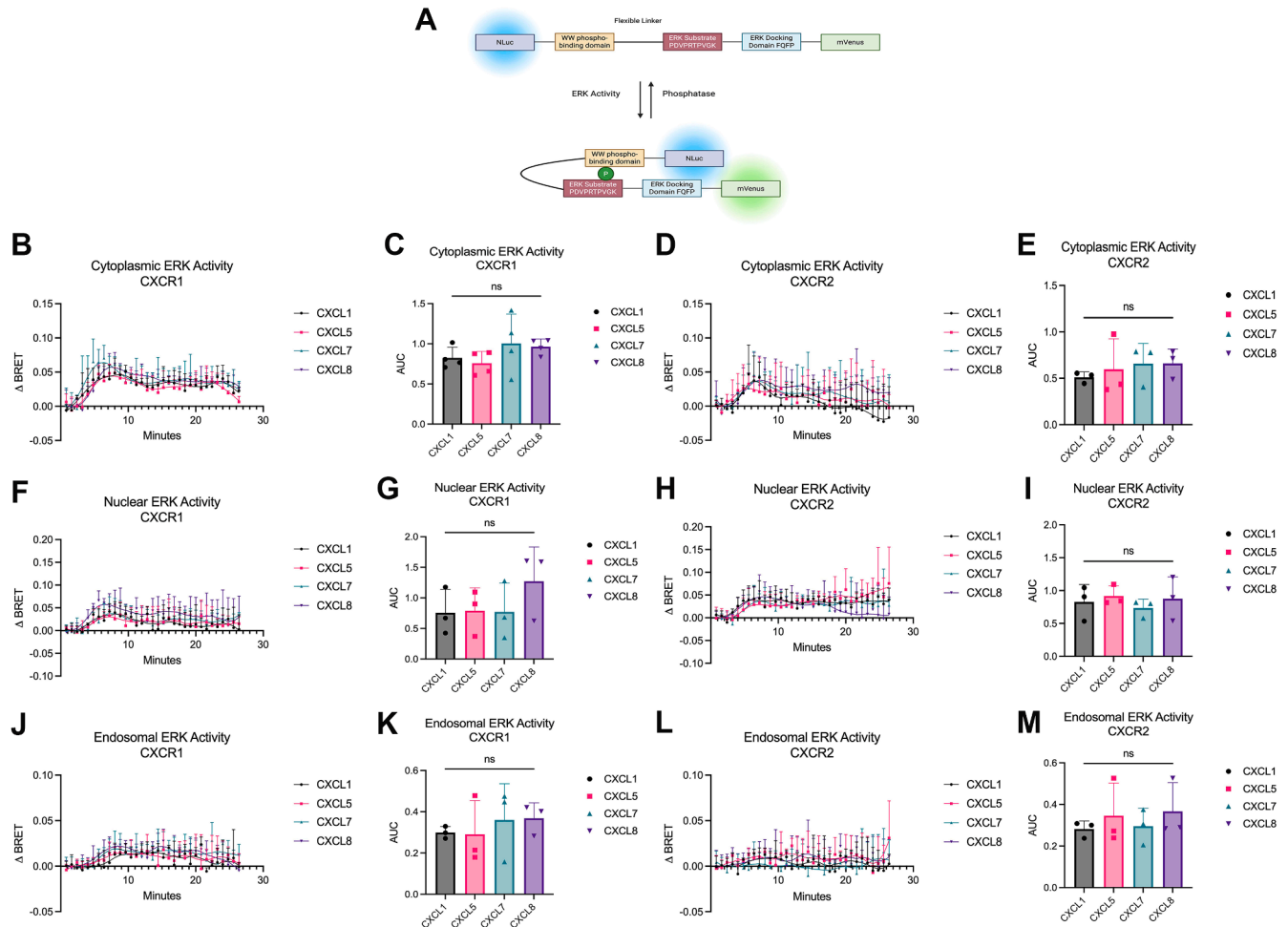


**Fig. 5.** CXCR1 and CXCR2 promote distinct ERK activation patterns at different subcellular locations. (A) Schematic of subcellular ERK activity reporter (EKAR) BRET targeted to the cytoplasm, the nucleus, and early endosomes to measure location-specific ERK activity induced by endogenous chemokines of CXCR1 and CXCR2 in HEK293T cells. (B, F, J) Time course data of cytoplasmic, nuclear, and endosomal ERK activity following stimulation of CXCR1 with 10  $\mu$ M of chemokine (C, G, K) with corresponding area under the curve (AUC) quantification. (D, H, L) Time course data of cytoplasmic, nuclear, and endosomal ERK activity following activation of CXCR2 with 10  $\mu$ M of chemokine (E, I, M) with corresponding AUC quantification. Data for (B) and (E) are the mean  $\pm$  SD ( $n = 4$ ) of independent plate-based experiments, and (C), (D), and (F–M) are the mean  $\pm$  SD ( $n = 3$ ) of independent plate-based experiments. For (E–G) and (K–M), a one-way ANOVA followed by Tukey's multiple comparison test was used to compare different chemokine treatments. ns:  $P \geq .05$ ; for effect of the ligand by one-way ANOVA. Created in BioRender. Jassal, C. (2026) <https://BioRender.com/3lell8c>.

As CXCR1 and CXCR2 predominantly couple to GRK2 and GRK6, respectively, to regulate neutrophil-mediated inflammatory responses,<sup>29</sup> we focused our studies on the recruitment of the GRK2/3 and GRK5/6 families to both receptors. We found that the rank order of chemokine-induced recruitment of GRK2 and GRK3 was similar to the trends observed in  $\beta$ -arrestin recruitment to CXCR1. However, no chemokine-dependent differences in GRK recruitment were observed following CXCR2 activation across the GRKs examined. Our data suggest that the interplay of receptor and chemokine bias at CXCR1 and CXCR2 may differentially modulate the functional output of unique GRK ensembles to produce unique phosphorylation barcodes at these receptors, as shown in previous studies at the CKR, CXCR3.<sup>30</sup> Exploring this further, we found that the involvement of GRK2/3 and GRK5/6 family members was conserved following CXCL8 stimulation at both receptors, whereas their roles were agonist-dependent for other chemokines, highlighting the ability of distinct ligands to confer unique functional properties to GRK family members.

Like many GPCRs, CXCR1 and CXCR2 have been shown to engage the mitogen-activated protein kinase pathway following treatment with CXCL8.<sup>11,27,29</sup> We expand on these findings to

include CXCL1, CXCL5, and CXCL7, further illuminating that these chemokines promote similar subcellular pools of ERK within the cytoplasm, nucleus, and endosomes. Moreover, it was appreciated that both G protein activation and receptor internalization contribute to promoting endosomal ERK for both CXCR1 and CXCR2. These findings enhance the granularity of signaling activity of CXCR1 and CXCR2 and their endogenous agonists through the lens of location-bias. Although the effects of receptor bias for CXCL1 were conserved in proximal signaling events, distal signaling outcomes appeared to be uncoupled from this bias. It is important to note some limitations of the data. We found that some of the chemokines, most notably CXCL5, displayed very low potency and efficacy at CXCR1 and CXCR2, raising the question as to whether a subset of ligands are authentic endogenous agonists of these receptors. Also, some of the performed experiments had a limited sample size, limiting their generalizability. Further studies are needed to assess the specific function of these unique signaling profiles in the context of mediating neutrophil activity during inflammatory responses.

Collectively, our findings establish a mechanistic framework in which receptor bias governs CXCL1 function, underlying distinct

biological roles for CXCR1 and CXCR2 through comparative analysis of shared chemokine agonists. Although the role of CXCL1 in driving neutrophil activity through CXCR2 has been extensively characterized,<sup>31–33</sup> its engagement of CXCR1 appears to be less defined. By directly comparing the responses of CXCR1 and CXCR2 to shared chemokine agonists, we reveal that receptor-specific bias governs signaling outcomes, most prominently in the context of CXCL1-mediated signaling. At CXCR1, bias favors weak transducer engagement and transient internalization, whereas at CXCR2, balanced  $\beta$ -arrestin and GRK engagement promotes sustained internalization events. These receptor-specific patterns suggest a mechanistic link between CXCL1 receptor bias and the nonredundant regulation of neutrophil activity by CXCR1 and CXCR2.

## Abbreviations

BRET, bioluminescence resonance energy transfer; KCR, chemokine receptor; CXCR1, C-X-C motif chemokine receptor 1; CXCR2, C-X-C motif chemokine receptor 2; GPCR, G protein-coupled receptor; GRK, G protein-coupled receptor kinase; HBSS, Hanks' balanced salt solution; KO, knockout; MEM, minimum essential media; P/S, penicillin/streptomycin; PEL, polyethylenimine; PTX, pertussis toxin; RLuc, *Renilla* luciferase.

## Acknowledgments

We thank Nour Nazo for laboratory assistance. Diagrams were made using BioRender.

## Financial support

S.R. is funded by R01 GM122798 and K.R. by NIH grants R21 AI160613 and a pilot grant from the UTMB Institute for Human Infections and Immunity.

## Conflict of interest

The authors declare no conflicts of interest.

## Data availability

The authors declare that all the data supporting the findings of this study are available within the paper and its [supplemental material](#).

## CRediT authorship contribution statement

**Chanpreet Jassal:** Conceptualization, Formal analysis, Investigation, Writing – original draft. **Joseph Strawn:** Conceptualization, Formal analysis, Investigation, Writing – original draft.

**Emily Walsh:** Investigation. **Krishna Rajarathnam:** Conceptualization, Funding acquisition, Resources, Supervision, Writing – review and editing. **Sudarshan Rajagopal:** Conceptualization, Funding acquisition, Resources, Supervision, Writing – review and editing.

## Supplemental material

This article has supplemental material available at [molpharm.aspetjournals.org](http://molpharm.aspetjournals.org).

## References

- Sriram K, Insel PA. G protein-coupled receptors as targets for approved drugs: how many targets and how many drugs? *Mol Pharmacol*. 2018;93(4):251–258. <https://doi.org/10.1124/mol.117.111062>
- Eiger DS, Pham U, Gardner J, Hicks C, Rajagopal S. GPCR systems pharmacology: a different perspective on the development of biased therapeutics. *Am J Physiol Cell Physiol*. 2022;322(5):C887–C895. <https://doi.org/10.1152/ajpcell.00449.2021>
- Rajagopal S, Rajagopal K, Lefkowitz RJ. Teaching old receptors new tricks: biasing seven-transmembrane receptors. *Nat Rev Drug Discov*. 2010;9(5):373–386. <https://doi.org/10.1038/nrd3024>
- Smith JS, Lefkowitz RJ, Rajagopal S. Biased signalling: from simple switches to allosteric microprocessors. *Nat Rev Drug Discov*. 2018;17(4):243–260. <https://doi.org/10.1038/nrd.2017.229>
- Schöneberg T, Schulz A, Biebermann H, Hermsdorf T, Römpler H, Sangkuhl K. Mutant G-protein-coupled receptors as a cause of human diseases. *Pharmacol Ther*. 2004;104(3):173–206. <https://doi.org/10.1016/j.pharmthera.2004.08.008>
- Eiger DS, Boldizar N, Honeycutt CC, Gardner J, Rajagopal S. Biased agonism at chemokine receptors. *Cell Signal*. 2021;78:109862. <https://doi.org/10.1016/j.celsig.2020.109862>
- Kohout TA, Nicholas SL, Perry SJ, Reinhart G, Junger S, Struthers RS. Differential desensitization, receptor phosphorylation,  $\beta$ -arrestin recruitment, and ERK1/2 activation by the two endogenous ligands for the CC chemokine receptor 7. *J Biol Chem*. 2004;279(22):23214–23222. <https://doi.org/10.1074/jbc.M402125200>
- Byers MA, Calloway PA, Shannon L, et al. Arrestin 3 mediates endocytosis of CCR7 following ligation of CCL19 but not CCL21. *J Immunol*. 2008;181(7):4723–4732. <https://doi.org/10.4049/jimmunol.181.7.4723>
- Zidar DA, Violin JD, Whalen EJ, Lefkowitz RJ. Selective engagement of G protein coupled receptor kinases (GRKs) encodes distinct functions of biased ligands. *Proc Natl Acad Sci U S A*. 2009;106(24):9649–9654. <https://doi.org/10.1073/pnas.0904361106>
- Rajagopal S, Kim J, Ahn S, et al. Beta-arrestin- but not G protein-mediated signaling by the "decoy" receptor CXCR7. *Proc Natl Acad Sci U S A*. 2010;107(2):628–632. <https://doi.org/10.1073/pnas.0912852107>
- Nasser MW, Raghuvanshi SK, Grant DJ, Jala VR, Rajarathnam K, Richardson RM. Differential activation and regulation of CXCR1 and CXCR2 by CXCL8 monomer and dimer. *J Immunol*. 2009;183(5):3425–3432. <https://doi.org/10.4049/jimmunol.0900305>
- Murphy PM, Tiffany HL. Cloning of complementary DNA encoding a functional human interleukin-8 receptor. *Science*. 1991;253(5025):1280–1283. <https://doi.org/10.1126/science.1891716>
- Ahuja SK, Lee JC, Murphy PM. CXC chemokines bind to unique sets of selectivity determinants that can function independently and are broadly distributed on multiple domains of human interleukin-8 receptor B. Determinants of high affinity binding and receptor activation are distinct. *J Biol Chem*. 1996;271(1):225–232. <https://doi.org/10.1074/jbc.271.1.225>
- Boon K, Vanalken N, Szpakowska M, Chevigné A, Schols D, Van Loy T. Systematic assessment of chemokine ligand bias at the human chemokine receptor CXCR2 indicates G protein bias over  $\beta$ -arrestin recruitment and receptor internalization. *Cell Commun Signal*. 2024;22(1):43. <https://doi.org/10.1186/s12964-023-01460-2>
- Boon K, Vanalken N, Szpakowska M, Chevigné A, Schols D, Van Loy T. High-affinity ELR+ chemokine ligands show G protein bias over  $\beta$ -arrestin recruitment and receptor internalization in CXCR1 signaling. *J Biol Chem*. 2025;301(1):108044. <https://doi.org/10.1016/j.jbc.2024.108044>
- Rajagopal S, Bassoni DL, Campbell JJ, Gerard NP, Gerard C, Wehrman TS. Biased agonism as a mechanism for differential signaling by chemokine receptors. *J Biol Chem*. 2013;288(49):35039–35048. <https://doi.org/10.1074/jbc.M113.479113>
- Bryksin AV, Matsumura I. Overlap extension PCR cloning: a simple and reliable way to create recombinant plasmids. *Biotechniques*. 2010;48(6):463–465. <https://doi.org/10.2144/000113418>
- Luttrell LM, Wang J, Plouffe B, et al. Manifold roles of  $\beta$ -arrestins in GPCR signaling elucidated with siRNA and CRISPR/Cas9. *Sci Signal*. 2018;11(549):eaat7650. <https://doi.org/10.1126/scisignal.aat7650>
- Kawakami K, Yanagawa M, Hiratsuka S, et al. Heterotrimeric Gq proteins act as a switch for GRK5/6 selectivity underlying  $\beta$ -arrestin transducer bias. *Nat Commun*. 2022;13(1):487. <https://doi.org/10.1038/s41467-022-28056-7>
- Olsen RHJ, DiBerto JF, English JG, et al. TRUPATH, an open-source biosensor platform for interrogating the GPCR transducerome. *Nat Chem Biol*. 2020;16(8):841–849. <https://doi.org/10.1038/s41589-020-0535-8>
- Wilson S, Wilkinson G, Milligan G. The CXCR1 and CXCR2 receptors form constitutive homo- and heterodimers selectively and with equal apparent affinities. *J Biol Chem*. 2005;280(31):28663–28674. <https://doi.org/10.1074/jbc.M413475200>
- Gardner J, Eiger DS, Hicks C, et al. GPCR kinases differentially modulate biased signaling downstream of CXCR3 depending on their subcellular localization. *Sci Signal*. 2024;17(823):eadd9139. <https://doi.org/10.1126/scisignal.add9139>
- Touhara K, Inglese J, Pitcher JA, Shaw G, Lefkowitz RJ. Binding of G protein  $\beta$ -subunits to pleckstrin homology domains. *J Biol Chem*. 1994;269(14):10217–10220. [https://doi.org/10.1016/S0021-9258\(17\)34048-6](https://doi.org/10.1016/S0021-9258(17)34048-6)
- Rajagopal S, Ahn S, Rominger DH, et al. Quantifying ligand bias at seven-transmembrane receptors. *Mol Pharmacol*. 2011;80(3):367–377. <https://doi.org/10.1124/mol.111.072801>

25. Pham U, Chundi A, Stepniwski TM, et al. Location-biased  $\beta$ -arrestin conformations direct GPCR signaling. Preprint. Posted online September 26. bioRxiv, 2024:2024.09.24.614742. <https://doi.org/10.1101/2024.09.24.614742>
26. Damke H, Baba T, Warnock DE, Schmid SL. Induction of mutant dynamin specifically blocks endocytic coated vesicle formation. *J Cell Biol.* 1994;127(4): 915–934. <https://doi.org/10.1083/jcb.127.4.915>
27. Prado GN, Suetomi K, Shumate D, et al. Chemokine signaling specificity: essential role for the N-terminal domain of chemokine receptors. *Biochemistry.* 2007;46(31):8961–8968. <https://doi.org/10.1021/bi7004043>
28. Rajarathnam K, Schnoor M, Richardson RM, Rajagopal S. How do chemokines navigate neutrophils to the target site: dissecting the structural mechanisms and signaling pathways. *Cell Signal.* 2019;54:69–80. <https://doi.org/10.1016/j.cellsig.2018.11.004>
29. Raghuvanshi SK, Su Y, Singh V, Haynes K, Richmond A, Richardson RM. The chemokine receptors CXCR1 and CXCR2 couple to distinct G protein-coupled receptor kinases to mediate and regulate leukocyte functions. *J Immunol.* 2012;189(6):2824–2832. <https://doi.org/10.4049/jimmunol.1201114>
30. Eiger DS, Smith JS, Shi T, et al. Phosphorylation barcodes direct biased chemokine signaling at CXCR3. Preprint. Posted online March 14, 2023. bioRxiv. 2023. 03.14.532634. <https://doi.org/10.1101/2023.03.14.532634>
31. Korbecki J, Bosiacki M, Barczak K, Łagocka R, Chlubek D, Baranowska-Bosiacka I. The clinical significance and role of CXCL1 chemokine in gastrointestinal cancers. *Cells.* 2023;12(10):1406. <https://doi.org/10.3390/cells12101406>
32. Sawant KV, Poluri KM, Dutta AK, et al. Chemokine CXCL1 mediated neutrophil recruitment: role of glycosaminoglycan interactions. *Sci Rep.* 2016;6:33123. <https://doi.org/10.1038/srep33123>
33. Ravindran A, Sawant KV, Sarmiento J, Navarro J, Rajarathnam K. Chemokine CXCL1 dimer is a potent agonist for the CXCR2 receptor. *J Biol Chem.* 2013;288(17):12244–12252. <https://doi.org/10.1074/jbc.M112.443762>